Letter

Magnetic ground state of the Kitaev $Na_2Co_2TeO_6$ spin liquid candidate

Weiliang Yao,[1,*] Yang Zhao,[2,3] Yiming Qiu,[2] Christian Balz,[4] J. Ross Stewart,[4] Jeffrey W. Lynn,[2] and Yuan Li[1,5,†]

[1]*International Center for Quantum Materials, School of Physics, Peking University, Beijing 100871, China*
[2]*NIST Center for Neutron Research, National Institute of Standards and Technology, Gaithersburg, Maryland 20899, USA*
[3]*Department of Materials Science and Engineering, University of Maryland, College Park, Maryland 20742, USA*
[4]*ISIS Neutron and Muon Source, STFC Rutherford Appleton Laboratory, Didcot OX11 0QX, United Kingdom*
[5]*Collaborative Innovation Center of Quantum Matter, Beijing 100871, China*

(Received 11 December 2022; revised 23 March 2023; accepted 11 May 2023; published 2 June 2023)

As a candidate Kitaev material, $Na_2Co_2TeO_6$ exhibits intriguing magnetism on a honeycomb lattice that is believed to be C_3 symmetric. Here we report a neutron diffraction study of high-quality single crystals under a-axis magnetic fields. Our data support the less common notion of a magnetic ground state that corresponds to a triple-**q** magnetic structure with C_3 symmetry, rather than the multidomain zigzag structure typically assumed in prototype Kitaev spin liquid candidates. In particular, we find that the field is unable to repopulate the supposed zigzag domains, where the only alternative explanation is that the domains are strongly pinned by hitherto unidentified structural reasons. If the triple-**q** structure is correct, then this requires reevaluation of many candidate Kitaev materials. We also find that fields beyond about 10 Tesla suppress the long-range antiferromagnetic order, allowing magnetic behavior to emerge different from that expected for a spin liquid.

DOI: 10.1103/PhysRevResearch.5.L022045

The exactly solvable Kitaev model [1] represents a distinct route to quantum many-body entanglement of spins [2] and has important potential for topological quantum computing [1,3]. Pursuit of Kitaev spin liquids (KSLs) [1] in crystalline materials has fueled intense research [4,5]. Among materialization ideas [4–8], several recently proposed cobalt oxides [9–12] are promising, since their $3d^7$ magnetic electrons are desirable for weakening non-Kitaev interactions [9,10]. Moreover, unlike α-$RuCl_3$ [13] and $H_3LiIr_2O_6$ [14], which are van der Waals materials, the cobaltates can be grown into large single crystals with relatively few imperfections [15–20].

An important common characteristic of the cobaltates and the $4d$-electron counterpart α-$RuCl_3$ is their tunability by magnetic fields. Such external tuning [21–25] is widely considered necessary for finding (field-driven) spin liquids, because most KSL candidate materials do have magnetic order at low temperature [4,5,8]. In α-$RuCl_3$, a hallmark of the tunability is field suppression of thermodynamic signatures of magnetic order [26,27], which has led to a flurry of studies of excitations in the intermediate and high-field states [28–38]. Indeed, similar field suppression of order and unconventional transport behaviors have been found in the cobaltates [16,17,19,20,39–44], which imply not only chances for finding spin liquids but also an experimental opportunity—brought by the high crystal quality—for elucidating the microscopic mechanisms. The latter aspect is significant because microscopic models of essentially *all* KSL candidate materials are currently under debate [39,45–57]. From an optimistic perspective, establishing a concrete case for at least one of them, despite the difficulty of the problem itself, may already provide valuable insight into many of the candidate materials.

Among the cobaltates, $Na_2Co_2TeO_6$ has been studied the most by spectroscopic methods [39,48–50,52,53,57–60]. Its crystal structure (space group $P6_322$) furthermore stands out among KSL candidate materials for having, at least nominally, threefold rotational (C_3) symmetry about the c axis [61–63], whereas many other materials have monoclinic stacking which removes the C_3 symmetry. Notably, C_3 is a symmetry that becomes broken in the presence of "zigzag" magnetic order [Fig. 1(a)], which is the most commonly considered form of order in KSL candidate materials [4,5]. The magnetic ground state of $Na_2Co_2TeO_6$ was initially reported to be zigzag based on neutron diffraction [62,63], which has also been used to identify zigzag order in other KSL candidate materials [19,64–66]. Recently, an alternative "triple-**q**" magnetic state [Fig. 1(b)] was suggested based on a distinct signature in the spin waves [58], which subsequently received indirect support from magnetic resonance [59,60]. The C_3-symmetric triple-**q** state can be constructed by adding zigzag components of three different orientations. For this reason, the triple-**q** and zigzag orders cannot be distinguished by diffraction [58], unless the C_3-symmetry breaking is revealed by observing uneven populations of its orientational domains. The C_3 structure of $Na_2Co_2TeO_6$ is desirable for this

*weiliangyao@outlook.com; Present address: Department of Physics and Astronomy, Rice University, Houston, TX 77005, USA.
†yuan.li@pku.edu.cn

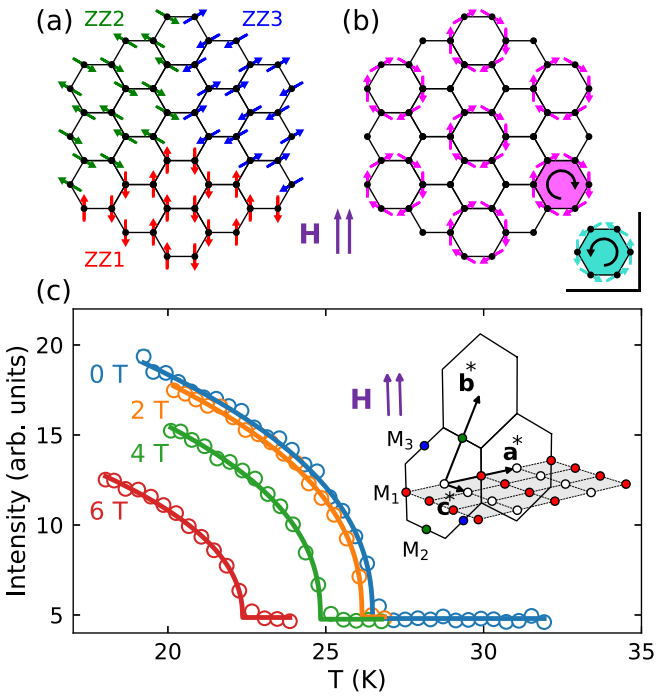

FIG. 1. (a) The zigzag magnetic structure and its orientational domains. (b) The triple-**q** magnetic structure. The moments can be thought of as a vector sum of the three patterns in panel (a) extended over the whole lattice. When one or three of the ZZ*n* components are reversed, the chirality is reversed (inset). (c) Temperature dependence of the M_1 (0.5, 0, 1) reflection in selected fields, where the long-range magnetic order is robust (see Fig. S3 in Ref. [71]). Solid curves are power-law fits to the data (see text). Inset shows the reciprocal lattice in our setting, where hexagons are boundaries of 2D Brillouin zones, and the shaded (H, 0, L) plane is perpendicular to the field (purple arrows). Empty circles are structural Brillouin zone centers. Filled circles are magnetic Bragg peaks at the M points, color coded with the zigzag domains in panel (a).

purpose, because a weak external perturbation (e.g., in-plane magnetic field, strain, etc.) can be expected to selectively populate the domains if the zigzag ground state is realized. Given the prominence of the zigzag order in KSL research, and since the magnetic ground-state symmetry fundamentally constrains our understanding of magnetotransport properties [41,42,44,67] and magnetic excitations [53,68], such an explicit test is much needed. Rigorous verification of the triple-**q** order in $Na_2Co_2TeO_6$ may further illuminate related research in other materials sharing the same crystal symmetry [69,70].

Here we report our magnetic neutron diffraction study of $Na_2Co_2TeO_6$ single crystals in order to test whether in-plane fields along the a axis can selectively populate magnetic domains. We also examine whether magnetic fields (up to 10 Tesla) can drive the system into a spin-disordered state, as has been previously suggested [16,39,40]. Our conclusion is that the fields can do neither of these. While a spin liquid might still be reachable with fields in other directions [57] and/or greater than 10 T, our results set a definitive constraint on the zero-field magnetic ground state. Namely, unless a lower structural symmetry without C_3 has previously been missed, the system prefers a C_3-symmetric triple-**q** state over the widely considered zigzag order.

Our experimental geometry is shown in the inset of Fig. 1(c). Magnetic Bragg peaks are expected at the M points of the two-dimensional (2D) Brillouin zone. They originate either separately from different zigzag domains [ZZ1–ZZ3 in Fig. 1(a), peaks at M_1–M_3, respectively], or together from the triple-**q** order. Figure 1(c) displays the temperature (T) dependence of the magnetic peak at M_1 (0.5, 0, 1). In the zigzag scenario, this peak arises from the ZZ1 domain, where the in-plane magnetic moments are collinear with the applied field [Fig. 1(a)]. The transition temperature ($T_N \approx 26.5$ K at 0 T) is gradually suppressed by the field, and the data can be fit with a power-law function: $I = A\,(T_N - T)^{2\beta} + B$, where A and B are scale and background constants, respectively, and β is the critical exponent of the order parameter, which changes very little from 0.209(7) to 0.227(13) between 0 and 6 T. This indicates that the nature of the magnetic transition barely changes with field and that it is different from the 2D Ising case found in α-$RuCl_3$ [30]. The deviation might be attributable to the fact that T_N marks three-dimensional ordering, which is preceded by a minor 2D transition at a slightly higher temperature [58]. The 2D transition cannot be observed in these data because of the small sample volume [71].

Figure 2(a) displays the system's field evolution as seen from the M_1 (0.5, 0, 1) magnetic peak at 2 K. Starting from an initial state prepared by zero-field cooling (ZFC), the intensity monotonically decreases with increasing field. Besides a subtle anomaly at about 1.5 T, the main decrease occurs between about 6 and 8.2 T, and a small but finite intensity remains at the highest field of 10 T, which we will revisit later. At first sight, the intensity decrease could be attributed to two reasons: (1) the antiferromagnetic order is suppressed by the field and (2) the zigzag domain ZZ1 responsible for the measured peak is unfavored by the field and gets transformed into ZZ2 and ZZ3. To test the relevance of (2), we continued our measurement upon removing and then reapplying the field. Intriguingly, the intensity recovers to about 2/3 of the original after the field is removed, and the sample appears to have entered a stable field-trained state—reapplying the field results in a field-dependent behavior different from the initial field application up to 8.2 T. The data further reveal a hysteretic behavior between 6 and 8.2 T. A cleaner procedure to prepare the field-trained state involves field-cooling (FC) the sample in a 10-T field and then removing the field.

A central issue here is whether or not the partial intensity loss in the field-trained state is due to domain repopulation. We first note that, with the structural C_3 symmetry, a sample prepared by FC can have no ZZ1 domain whatsoever, but this view is defied by the 2/3-recovered intensity. In Fig. 2(b), we present data measured on an integer-indexed peak (1, 0, 1), which show that the field-trained state is *not* different from the ZFC state as far as uniform magnetization and susceptibility are concerned—the intensity and its field derivative at 0 T both recover to the original values. Since the zigzag domains have different susceptibility in a given field direction, this result implies that there is no zigzag domain repopulation after the field is removed. As a further test, Fig. 2(c) displays the field evolution of the M_2 (0, 0.5, 1) peak, which is associated with domain ZZ2 in the zigzag scenario (see Fig. S4 in Ref. [71]

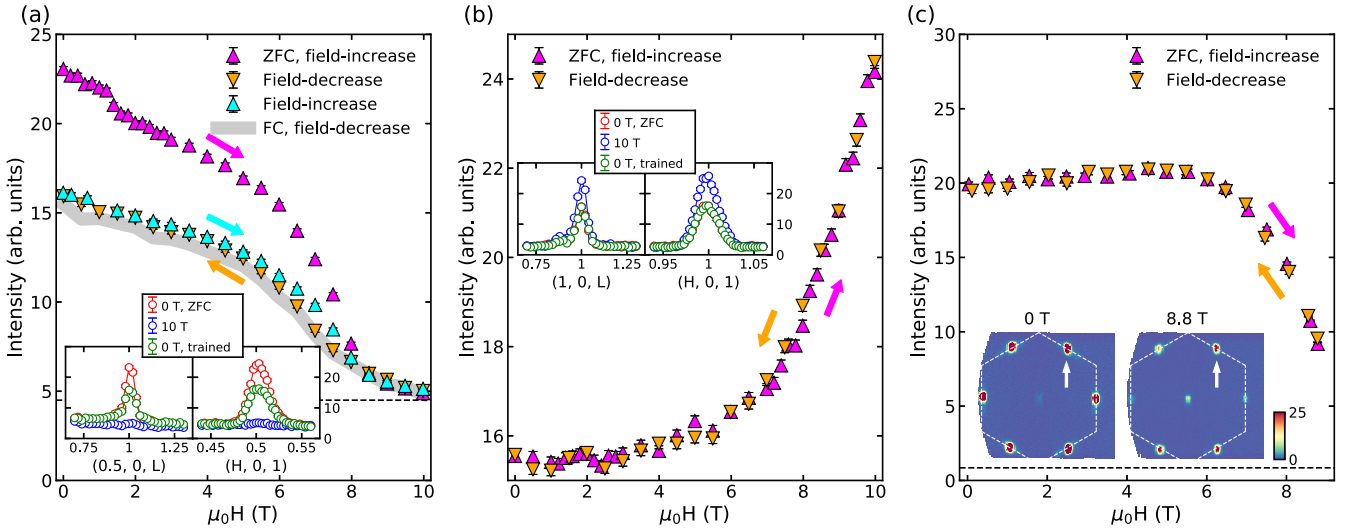

FIG. 2. (a) Field evolution of magnetic Bragg peak M_1 (0.5, 0, 1) at 2 K, with the sample undergoing a series of field scans after zero-field cooling (ZFC, see text), as well as after field cooling (FC) in 10 T. (b) Field evolution of Bragg peak (1, 0, 1) at 2 K. In the virgin zero field state, the observed intensity is due to nuclear Bragg scattering, whereas the field-enhanced intensity is a measure of uniform magnetization. (c) Field evolution of magnetic Bragg peak M_2 (0, 0.5, 1) at 2 K. Measurements displayed in the main panels are performed at the maximum of the peak profiles displayed in the insets. Horizontal dashed lines in panels (a) and (c) indicate background level. Error bars indicate statistical uncertainty (1 s.d.).

for similar result for the M_3 peak). While the behavior is qualitatively different from the M_1 peak below 6 T, there is no intensity gain on M_2 in the field-trained state. We thus conclude that the loss of the M_1 peak intensity is unrelated to domain repopulation. In this context, we note that some previous related results in α-$RuCl_3$ [26,33] have been attributed to zigzag-domain repopulation by small in-plane fields. Those results are qualitatively similar to our data obtained upon the initial field application in Figs. 2(a) and 2(c), and the interpretation was made even in the absence of C_3 structural symmetry of α-$RuCl_3$. As the structural symmetry is expected to make the zigzag domains energetically unequal, it follows that the magnetization energy must be able to overcome the difference. In this sense, our results in $Na_2Co_2TeO_6$ are particularly difficult to comprehend under the zigzag scenario, because the structural C_3 symmetry should make the magnetic domains even easier to repopulate than in α-$RuCl_3$.

To reveal where the lost intensity of M_1 (0.5, 0, 1) has gone in the field-trained state, Figs. 3(a)–3(c) present our measurement in an extensive region of the $(H, 0, L)$ reciprocal plane. After ZFC, a rod of magnetic scattering running along $\mathbf{c}^*$ is observed at $H = 0.5$, in addition to the sharp peaks at integer L. It signifies quasi-2D magnetic correlations [58], and the signal becomes noticeably enhanced in the field-trained state [Figs. 3(c) and 3(d)]. The enhancement occurs upon decreasing the field between 8.2 and 6 T (Fig. S5 in Ref. [71]) and can approximately account for the intensity loss at integer L (Fig. S9 in Ref. [71]). Therefore, field training suppresses c-axis correlations, but it leaves the L-integrated 2D diffraction signal at M_1 (0.5, 0) unaffected. This reinforces our conclusion of no zigzag domain repopulation. The field training leaves no significant change in the 2D correlation length [Fig. 2(a) inset], or in the c-axis correlations characterized by $M_{2,3}$ [Fig. 2(c)]. Moreover, the lost c-axis correlations at M_1 (0.5, 0, 1) can be partially recovered [Fig. 3(e)] by warming up the field-trained sample. The implication of these observations will be discussed later. We note that the system behaves somewhat differently from α-$RuCl_3$, where a distinct form of magnetic order perpendicular to the honeycomb plane can be stabilized by intermediate in-plane fields [72],

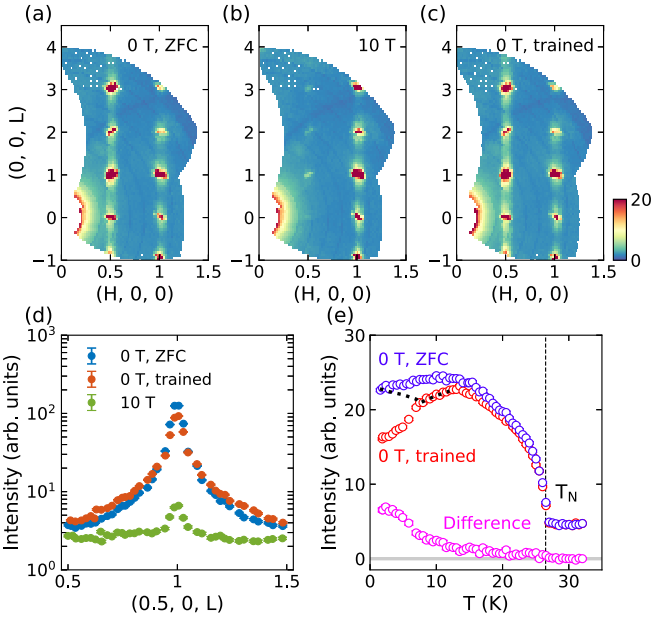

FIG. 3. [(a)–(c)] Elastic scattering in the $(H, 0, L)$ plane measured at 0.1 K under the specified field conditions. (d) Line cuts through the data in panels (a)–(c) along $\mathbf{c}^*$ at $H = 0.5$. (e) T dependence of the signal at M_1 (0.5, 0, 1) measured in zero field upon warming the sample, before and after field training. Black dotted curve illustrates expected T dependence of the M_2 (0, 0.5, 1) and M_3 (−0.5, 0.5, 1) signals after field training, if the triple-$\mathbf{q}$ scenario is correct (see text).

presumably due to a more significant role of the system's interplane coupling [35].

Comparing the data in Figs. 3(a) and 3(b), we notice enhanced scattering at integer H and L at 10 T, where no magnetic scattering exists at 0 T (Fig. S7 in Ref. [71]). This additional signal is therefore purely due to field-induced uniform magnetization. An induced moment of about 2.05(3) μ_B/Co can be estimated from the data [71], consistent with previous reports [39,43]. While this means that the field suppresses antiferromagnetic order by causing significant spin polarization, the peaks at $H = 0.5$ are not fully suppressed [Figs. 3(b) and 3(d)], and their magnetic nature has been confirmed by comparing to measurements at high temperature (Fig. S8 in Ref. [71]). The system is always in a magnetically ordered state under a-axis fields up to 10 T, and is therefore not yet a spin liquid. Nevertheless, recent studies of $Na_2Co_2TeO_6$ have revealed unusual thermal transport properties under in-plane fields, which implies that the near-polarized state is distinct from a conventional paramagnet [40,44]. Similar behaviors are also observed in $BaCo_2(AsO_4)_2$ [17], where both Kitaev and non-Kitaev scenarios have been put forward to interpret the experimental data [17,18,51,73,74]. These studies motivate further searches for exotic magnetism in the cobalt-based honeycomb materials.

We now discuss possible scenarios for the field training to cause no diffraction intensity transfer between the M points. In the first scenario, the M points are associated with spatially separated zigzag domains, as we illustrate in the upper half of Fig. 4(a). In order for the field training not to repopulate the domains, they must be completely pinned by the local crystal lattice regarding their zigzag-chain orientations. Given the high quality of our crystals as indicated by the highly uniform value of T_N [16,53,71], the sharp magnetic transition at T_N [Fig. 1(c)] and the well-defined crystal mosaic (Fig. S7 [71]), we believe that such pinning is not due to structural defects or disorder in the Na layers [62,63]. It can only be rationalized if the crystal structure features a hitherto unnoticed breaking of the C_3 symmetry, e.g., due to the stacking of the layers [66,75,76]. We note that the crystal structure has some subtleties, including an in-plane superstructure previously seen by single-crystal neutron and x-ray diffraction [58]. However, any genuine breaking of the C_3 symmetry ought to result in unequal a- and b-axis lattice constants and a splitting of the powder diffraction peaks, which has not been observed experimentally [15,39,49,62,63]. We therefore consider this scenario rather unlikely. In the second scenario, as illustrated in the lower half of Fig. 4(a), the M points all belong to the same triple-**q** order parameter, which naturally explains the lack of opportunity for orientational domain repopulation.

To this end, the field-training effect on the c-axis correlations deserves some thought. Given that the effect is only observed at M_1 [Figs. 2(a) and 2(c)], we illustrate plausible changes caused by the training in Figs. 4(b) and 4(c) and Figs. 4(d) and 4(e), respectively, for the zigzag and the triple-**q** cases. In the former case, the interlayer arrangement inside the ZZ1 domain is disturbed by the training, probably because the field causes a spin-flop-like transition between 6 and 8.2 T, as the hysteretic behavior [Fig. 2(a)] suggests. Indeed, the first-order nature of the transition is expected to strongly

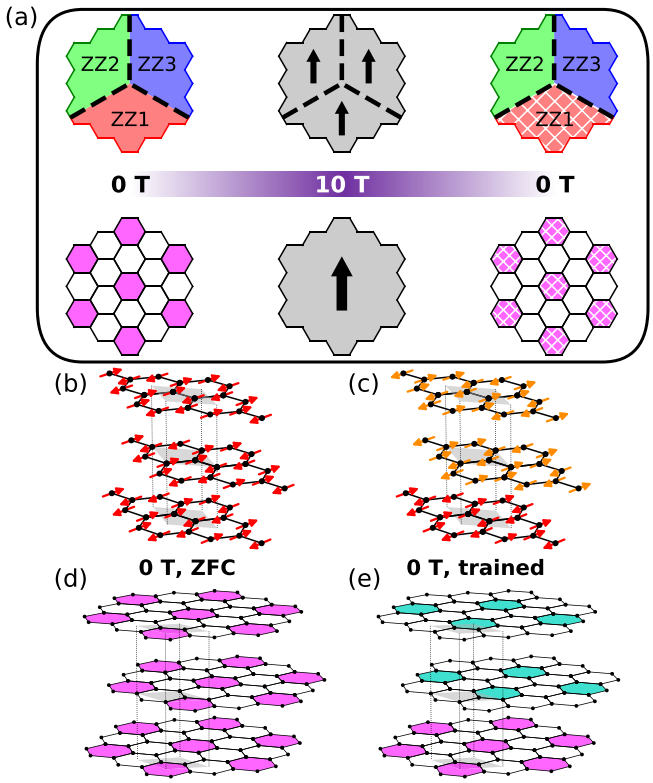

FIG. 4. (a) Schematic field-training processes under the zigzag (upper half) and triple-**q** (lower half) scenarios. The 10-T state is approximated as fully spin polarized. Polygons are color coded with Figs. 1(a) and 1(b). Dashed lines are boundaries between "hidden" low-symmetry structural domains. Hatches indicate suppressed c-axis correlations. [(b), (c)] Schematic stacking in the (supposed) ZZ1 domain before and after field training. Yellow arrows indicate randomly reversed layers. [(d), (e)] Schematic stacking in the triple-**q** structure before and after field training, color coded after Fig. 1(b). Gray rhombuses in panels (b)–(e) indicate the structural primitive cell.

disturb ZZ1, but it would naturally leave ZZ2 and ZZ3 intact. In the latter case, we note that inside a given honeycomb layer, reversing one zigzag component in the triple-**q** structure would reverse the layer's spin chirality [Fig. 1(b)]. Hence, the suppressed c-axis correlations at M_1, but not at M_2 or M_3, imply a scrambled arrangement of the chirality across the layers [Figs. 4(d) and 4(e)]. Importantly, the fact that warming up a field-trained sample recovers part of the c-axis correlations seen at M_1, as shown in Fig. 3(e), also has very different explanations in the two cases. In the zigzag case, the recovery pertains to only the ZZ1 domain, which means that the diffraction signals at M_2 and M_3 will not be affected. Since the latter signals are the same in the ZFC and field-trained states [Fig. 2(c)], upon warming the sample from 2 K, they are expected to simply follow the ZFC curve in Fig. 3(e). In contrast, in the triple-**q** case, the scrambled chirality between the layers is not expected to recover easily by thermal fluctuations. Instead, the pattern in each layer might be able to translate, which corresponds to reversing *two* zigzag components simultaneously (Fig. S10 in Ref. [71]). Mathematically, such a process would partially recover the c-axis correlations seen at M_1, but at the cost of the correlations at M_2 and M_3.

It means that if one can monitor, e.g., the M_2 (0, 0.5, 1) peak upon warming the sample from a field-trained state, the measured intensity would be like the dotted lines in Fig. 3(e). Such a distinct behavior from the zigzag case, if confirmed in future studies, will firmly establish the triple-**q** scenario. In fact, we believe that such crosstalk between signals at different wave vectors can be utilized, on very general grounds indeed, for experimental differentiation between single- and multi-**q** magnetic orders regardless of the crystal structure. The experiment requires a demanding condition with both a magnet and detector coverage for observing the out-of-horizontal-plane diffraction peaks.

To conclude, we have investigated the a-axis field dependence of magnetic order in $Na_2Co_2TeO_6$ with neutron diffraction. In spite of the nominal C_3 crystal symmetry, we find that an a-axis applied field is unable to repopulate C_3-breaking magnetic domains—either such domains exist but are completely pinned by an as yet unknown (and unlikely) low-symmetry structure, or the magnetic ground state features the C_3-symmetric triple-**q** structure. Our study brings unprecedented insight into the crystal and magnetic structures of not only $Na_2Co_2TeO_6$, but also related systems with presumed zigzag order that may actually be triple-**q**. Finally, we show that $Na_2Co_2TeO_6$ is not yet a spin liquid up to 10 T, but its magnetism remains highly intriguing and awaits further elucidation.

We are grateful for discussions with L. Chen, W. Chen, C. Hess, X. Hong, L. Janssen, X. Jin, D. Khalyavin, C. Kim, V. Kocsis, W. G. F. Krüger, J.-G. Park, L. Taillefer, and A. U. B. Wolter. The work at Peking University was supported by the National Basic Research Program of China (Grant No. 2021YFA1401900) and the National Natural Science Foundation of China (Grants No. 12061131004 and No. 11888101). Access to MACS was provided by the Center for High Resolution Neutron Scattering, a partnership between the National Institute of Standards and Technology and the National Science Foundation under Agreement No. DMR-1508249. We acknowledge ISIS for beam time under Proposal No. RB2010025 [77].

[1] A. Kitaev, Anyons in an exactly solved model and beyond, Ann. Phys. **321**, 2 (2006).

[2] P. W. Anderson, Resonating valence bonds: A new kind of insulator?, Mater. Res. Bull. **8**, 153 (1973).

[3] C. Nayak, S. H. Simon, A. Stern, M. Freedman, and S. Das Sarma, Non-Abelian anyons and topological quantum computation, Rev. Mod. Phys. **80**, 1083 (2008).

[4] H. Takagi, T. Takayama, G. Jackeli, G. Khaliullin, and S. E. Nagler, Concept and realization of Kitaev quantum spin liquids, Nat. Rev. Phys. **1**, 264 (2019).

[5] S. Trebst and C. Hickey, Kitaev materials, Phys. Rep. **950**, 1 (2022).

[6] G. Jackeli and G. Khaliullin, Mott Insulators in the Strong Spin-Orbit Coupling Limit: From Heisenberg to a Quantum Compass and Kitaev Models, Phys. Rev. Lett. **102**, 017205 (2009).

[7] J. Chaloupka, G. Jackeli, and G. Khaliullin, Kitaev-Heisenberg Model on a Honeycomb Lattice: Possible Exotic Phases in Iridium Oxides A_2IrO_3, Phys. Rev. Lett. **105**, 027204 (2010).

[8] S. M. Winter, A. A. Tsirlin, M. Daghofer, J. van den Brink, Y. Singh, P. Gegenwart, and R. Valentí, Models and materials for generalized Kitaev magnetism, J. Phys.: Condens. Matter **29**, 493002 (2017).

[9] H. Liu and G. Khaliullin, Pseudospin exchange interactions in d^7 cobalt compounds: Possible realization of the Kitaev model, Phys. Rev. B **97**, 014407 (2018).

[10] R. Sano, Y. Kato, and Y. Motome, Kitaev-Heisenberg Hamiltonian for high-spin d^7 Mott insulators, Phys. Rev. B **97**, 014408 (2018).

[11] Y. Motome, R. Sano, S. Jang, Y. Sugita, and Y. Kato, Materials design of Kitaev spin liquids beyond the Jackeli–Khaliullin mechanism, J. Phys.: Condens. Matter **32**, 404001 (2020).

[12] C. Kim, H.-S. Kim, and J.-G. Park, Spin-orbital entangled state and realization of Kitaev physics in 3d cobalt compounds: A progress report, J. Phys.: Condens. Matter **34**, 023001 (2022).

[13] K. W. Plumb, J. P. Clancy, L. J. Sandilands, V. V. Shankar, Y. F. Hu, K. S. Burch, H.-Y. Kee, and Y.-J. Kim, α-$RuCl_3$: A spin-orbit assisted Mott insulator on a honeycomb lattice, Phys. Rev. B **90**, 041112(R) (2014).

[14] K. Kitagawa, T. Takayama, Y. Matsumoto, A. Kato, R. Takano, Y. Kishimoto, S. Bette, R. Dinnebier, G. Jackeli, and H. Takagi, A spin-orbital-entangled quantum liquid on a honeycomb lattice, Nature (London) **554**, 341 (2018).

[15] G. Xiao, Z. Xia, W. Zhang, X. Yue, S. Huang, X. Zhang, F. Yang, Y. Song, M. Wei, H. Deng, and D. Jiang, Crystal growth and the magnetic properties of $Na_2Co_2TeO_6$ with quasi-two-dimensional honeycomb lattice, Cryst. Growth Des. **19**, 2658 (2019).

[16] W. Yao and Y. Li, Ferrimagnetism and anisotropic phase tunability by magnetic fields in $Na_2Co_2TeO_6$, Phys. Rev. B **101**, 085120 (2020).

[17] R. Zhong, T. Gao, N. P. Ong, and R. J. Cava, Weak-field induced nonmagnetic state in a Co-based honeycomb, Sci. Adv. **6**, eaay6953 (2020).

[18] T. Halloran, F. Desrochers, E. Z. Zhang, T. Chen, L. E. Chern, Z. Xu, B. Winn, M. Graves-Brook, M. B. Stone, A. I. Kolesnikov, Y. Qiu, R. Zhong, R. Cava, Y. B. Kim, and C. Broholm, Geometrical frustration versus Kitaev interactions in $BaCo_2(AsO_4)_2$, Proc. Natl. Acad. Sci. USA **120**, e2215509119 (2023).

[19] J.-Q. Yan, S. Okamoto, Y. Wu, Q. Zheng, H. D. Zhou, H. B. Cao, and M. A. McGuire, Magnetic order in single crystals of $Na_3Co_2SbO_6$ with a honeycomb arrangement of $3d^7$ Co^{2+} ions, Phys. Rev. Mater. **3**, 074405 (2019).

[20] X. Li, Y. Gu, Y. Chen, V. O. Garlea, K. Iida, K. Kamazawa, Y. Li, G. Deng, Q. Xiao, X. Zheng, Z. Ye, Y. Peng, I. A. Zaliznyak, J. M. Tranquada, and Y. Li, Giant Magnetic in-Plane Anisotropy and Competing Instabilities in $Na_3Co_2SbO_6$, Phys. Rev. X **12**, 041024 (2022).

[21] L. Janssen, E. C. Andrade, and M. Vojta, Honeycomb-Lattice Heisenberg-Kitaev Model in a Magnetic Field: Spin Canting, Metamagnetism, and Vortex Crystals, Phys. Rev. Lett. **117**, 277202 (2016).

[22] L. Janssen and M. Vojta, Heisenberg–Kitaev physics in magnetic fields, J. Phys.: Condens. Matter **31**, 423002 (2019).

[23] J. S. Gordon, A. Catuneanu, E. S. Sørensen, and H.-Y. Kee, Theory of the field-revealed Kitaev spin liquid, Nat. Commun. **10**, 2470 (2019).

[24] C. Hickey and S. Trebst, Emergence of a field-driven $U(1)$ spin liquid in the Kitaev honeycomb model, Nat. Commun. **10**, 530 (2019).

[25] H. Li, H.-K. Zhang, J. Wang, H.-Q. Wu, Y. Gao, D.-W. Qu, Z.-X. Liu, S.-S. Gong, and W. Li, Identification of magnetic interactions and high-field quantum spin liquid in α-$RuCl_3$, Nat. Commun. **12**, 4007 (2021).

[26] J. A. Sears, Y. Zhao, Z. Xu, J. W. Lynn, and Y.-J. Kim, Phase diagram of α-$RuCl_3$ in an in-plane magnetic field, Phys. Rev. B **95**, 180411(R) (2017).

[27] A. U. B. Wolter, L. T. Corredor, L. Janssen, K. Nenkov, S. Schönecker, S.-H. Do, K.-Y. Choi, R. Albrecht, J. Hunger, T. Doert, M. Vojta, and B. Büchner, Field-induced quantum criticality in the Kitaev system α-$RuCl_3$, Phys. Rev. B **96**, 041405(R) (2017).

[28] S.-H. Baek, S.-H. Do, K.-Y. Choi, Y. S. Kwon, A. U. B. Wolter, S. Nishimoto, J. van den Brink, and B. Büchner, Evidence for a Field-Induced Quantum Spin Liquid in α-$RuCl_3$, Phys. Rev. Lett. **119**, 037201 (2017).

[29] J. Zheng, K. Ran, T. Li, J. Wang, P. Wang, B. Liu, Z.-X. Liu, B. Normand, J. Wen, and W. Yu, Gapless Spin Excitations in the Field-Induced Quantum Spin Liquid Phase of α-$RuCl_3$, Phys. Rev. Lett. **119**, 227208 (2017).

[30] A. Banerjee, J. Yan, J. Knolle, C. A. Bridges, M. B. Stone, M. D. Lumsden, D. G. Mandrus, D. A. Tennant, R. Moessner, and S. E. Nagler, Neutron scattering in the proximate quantum spin liquid α-$RuCl_3$, Science **356**, 1055 (2017).

[31] S.-H. Do, S.-Y. Park, J. Yoshitake, J. Nasu, Y. Motome, Y. S. Kwon, D. Adroja, D. Voneshen, K. Kim, T.-H. Jang, J.-H. Park, K.-Y. Choi, and S. Ji, Majorana fermions in the Kitaev quantum spin system α-$RuCl_3$, Nat. Phys. **13**, 1079 (2017).

[32] Y. Kasahara, T. Ohnishi, Y. Mizukami, O. Tanaka, S. Ma, K. Sugii, N. Kurita, H. Tanaka, J. Nasu, Y. Motome, T. Shibauchi, and Y. Matsuda, Majorana quantization and half-integer thermal quantum Hall effect in a Kitaev spin liquid, Nature (London) **559**, 227 (2018).

[33] A. Banerjee, P. Lampen-Kelley, J. Knolle, C. Balz, A. A. Aczel, B. Winn, Y. Liu, D. Pajerowski, J. Yan, C. A. Bridges, A. T. Savici, B. C. Chakoumakos, M. D. Lumsden, D. A. Tennant, R. Moessner, D. G. Mandrus, and S. E. Nagler, Excitations in the field-induced quantum spin liquid state of α-$RuCl_3$, npj Quantum Mater. **3**, 8 (2018).

[34] R. Hentrich, A. U. B. Wolter, X. Zotos, W. Brenig, D. Nowak, A. Isaeva, T. Doert, A. Banerjee, P. Lampen-Kelley, D. G. Mandrus, S. E. Nagler, J. Sears, Y.-J. Kim, B. Büchner, and C. Hess, Unusual Phonon Heat Transport in α-$RuCl_3$: Strong Spin-Phonon Scattering and Field-Induced Spin Gap, Phys. Rev. Lett. **120**, 117204 (2018).

[35] C. Balz, P. Lampen-Kelley, A. Banerjee, J. Yan, Z. Lu, X. Hu, S. M. Yadav, Y. Takano, Y. Liu, D. A. Tennant, M. D. Lumsden, D. Mandrus, and S. E. Nagler, Finite field regime for a quantum spin liquid in α-$RuCl_3$, Phys. Rev. B **100**, 060405(R) (2019).

[36] T. Yokoi, S. Ma, Y. Kasahara, S. Kasahara, T. Shibauchi, N. Kurita, H. Tanaka, J. Nasu, Y. Motome, C. Hickey, S. Trebst, and Y. Matsuda, Half-integer quantized anomalous thermal Hall effect in the Kitaev material candidate α-$RuCl_3$, Science **373**, 568 (2021).

[37] J. A. N. Bruin, R. R. Claus, Y. Matsumoto, N. Kurita, H. Tanaka, and H. Takagi, Robustness of the thermal Hall effect close to half-quantization in α-$RuCl_3$, Nat. Phys. **18**, 401 (2022).

[38] E. Lefrançois, G. Grissonnanche, J. Baglo, P. Lampen-Kelley, J.-Q. Yan, C. Balz, D. Mandrus, S. E. Nagler, S. Kim, Y.-J. Kim, N. Doiron-Leyraud, and L. Taillefer, Evidence of a phonon Hall effect in the Kitaev spin liquid candidate α-$RuCl_3$, Phys. Rev. X **12**, 021025 (2022).

[39] G. Lin, J. Jeong, C. Kim, Y. Wang, Q. Huang, T. Masuda, S. Asai, S. Itoh, G. Günther, M. Russina, Z. Lu, J. Sheng, L. Wang, J. Wang, G. Wang, Q. Ren, C. Xi, W. Tong, L. Ling, Z. Liu, L. Wu, J. Mei, Z. Qu, H. Zhou, X. Wang, J.-G. Park, Y. Wan, and J. Ma, Field-induced quantum spin disordered state in spin-1/2 honeycomb magnet $Na_2Co_2TeO_6$, Nat. Commun. **12**, 5559 (2021).

[40] X. Hong, M. Gillig, R. Hentrich, W. Yao, V. Kocsis, A. R. Witte, T. Schreiner, D. Baumann, N. Pérez, A. U. B. Wolter, Y. Li, B. Büchner, and C. Hess, Strongly scattered phonon heat transport of the candidate Kitaev material $Na_2Co_2TeO_6$, Phys. Rev. B **104**, 144426 (2021).

[41] N. Li, S. Guang, W. Chu, Q. Huang, J. Liu, K. Xia, X. Zhou, X. Yue, Y. Sun, Y. Wang, Q. Li, G. Lin, J. Ma, X. Zhao, H. Zhou, and X. Sun, Sign switchable magnon thermal Hall conductivity in an antiferromagnet, arXiv:2201.11396.

[42] H. Yang, C. Kim, Y. Choi, J. H. Lee, G. Lin, J. Ma, M. Kratochvílová, P. Proschek, E.-G. Moon, K. H. Lee, Y. S. Oh, and J.-G. Park, Significant thermal Hall effect in the $3d$ cobalt Kitaev system $Na_2Co_2TeO_6$, Phys. Rev. B **106**, L081116 (2022).

[43] G. Xiao, Z. Xia, Y. Song, and L. Xiao, Magnetic properties and phase diagram of quasi-two-dimensional $Na_2Co_2TeO_6$ single crystal under high magnetic field, J. Phys.: Condens. Matter **34**, 075801 (2022).

[44] H. Takeda, J. Mai, M. Akazawa, K. Tamura, J. Yan, K. Moovendaran, K. Raju, R. Sankar, K.-Y. Choi, and M. Yamashita, Planar thermal Hall effects in the Kitaev spin liquid candidate $Na_2Co_2TeO_6$, Phys. Rev. Res. **4**, L042035 (2022).

[45] J. Rusnačko, D. Gotfryd, and J. Chaloupka, Kitaev-like honeycomb magnets: Global phase behavior and emergent effective models, Phys. Rev. B **99**, 064425 (2019).

[46] P. A. Maksimov and A. L. Chernyshev, Rethinking α-$RuCl_3$, Phys. Rev. Res. **2**, 033011 (2020).

[47] P. Laurell and S. Okamoto, Dynamical and thermal magnetic properties of the Kitaev spin liquid candidate α-$RuCl_3$, npj Quantum Mater. **5**, 2 (2020).

[48] M. Songvilay, J. Robert, S. Petit, J. A. Rodriguez-Rivera, W. D. Ratcliff, F. Damay, V. Balédent, M. Jiménez-Ruiz, P. Lejay, E. Pachoud, A. Hadj-Azzem, V. Simonet, and C. Stock, Kitaev interactions in the Co honeycomb antiferromagnets $Na_3Co_2SbO_6$ and $Na_2Co_2TeO_6$, Phys. Rev. B **102**, 224429 (2020).

[49] A. M. Samarakoon, Q. Chen, H. Zhou, and V. O. Garlea, Static and dynamic magnetic properties of honeycomb lattice antiferromagnets $Na_2M_2TeO_6$, M = Co and Ni, Phys. Rev. B **104**, 184415 (2021).

[50] C. Kim, J. Jeong, G. Lin, P. Park, T. Masuda, S. Asai, S. Itoh, H.-S. Kim, H. Zhou, J. Ma, and J.-G. Park, Antiferromagnetic Kitaev interaction in $J_{\text{eff}} = 1/2$ cobalt honeycomb materials

$Na_3Co_2SbO_6$ and $Na_2Co_2TeO_6$, J. Phys.: Condens. Matter **34**, 045802 (2022).

[51] S. Das, S. Voleti, T. Saha-Dasgupta, and A. Paramekanti, XY magnetism, Kitaev exchange, and long-range frustration in the $J_{\rm eff} = \frac{1}{2}$ honeycomb cobaltates, Phys. Rev. B **104**, 134425 (2021).

[52] A. L. Sanders, R. A. Mole, J. Liu, A. J. Brown, D. Yu, C. D. Ling, and S. Rachel, Dominant Kitaev interactions in the honeycomb materials $Na_3Co_2SbO_6$ and $Na_2Co_2TeO_6$, Phys. Rev. B **106**, 014413 (2022).

[53] W. Yao, K. Iida, K. Kamazawa, and Y. Li, Excitations in the Ordered and Paramagnetic States of Honeycomb Magnet $Na_2Co_2TeO_6$, Phys. Rev. Lett. **129**, 147202 (2022).

[54] S. M. Winter, Magnetic couplings in edge-sharing high-spin d^7 compounds, J. Phys.: Mater. **5**, 045003 (2022).

[55] P. A. Maksimov, A. V. Ushakov, Z. V. Pchelkina, Y. Li, S. M. Winter, and S. V. Streltsov, *Ab initio* guided minimal model for the "Kitaev" material $BaCo_2(AsO_4)_2$: Importance of direct hopping, third-neighbor exchange, and quantum fluctuations, Phys. Rev. B **106**, 165131 (2022).

[56] S. K. Pandey and J. Feng, Spin interaction and magnetism in cobaltate Kitaev candidate materials: An *ab initio* and model Hamiltonian approach, Phys. Rev. B **106**, 174411 (2022).

[57] G. Lin, Q. Zhao, G. Li, M. Shu, Y. Ma, J. Jiao, Q. Huang, J. Sheng, A. Kolesnikov, L. Li, L. Wu, X. Wang, H. Zhou, Z. Liu, and J. Ma, Evidence for field induced quantum spin liquid behavior in a spin-1/2 honeycomb magnet, Research Square (2022).

[58] W. Chen, X. Li, Z. Hu, Z. Hu, L. Yue, R. Sutarto, F. He, K. Iida, K. Kamazawa, W. Yu, X. Lin, and Y. Li, Spin-orbit phase behavior of $Na_2Co_2TeO_6$ at low temperatures, Phys. Rev. B **103**, L180404 (2021).

[59] C. H. Lee, S. Lee, Y. S. Choi, Z. H. Jang, R. Kalaivanan, R. Sankar, and K.-Y. Choi, Multistage development of anisotropic magnetic correlations in the Co-based honeycomb lattice $Na_2Co_2TeO_6$, Phys. Rev. B **103**, 214447 (2021).

[60] J. Kikuchi, T. Kamoda, N. Mera, Y. Takahashi, K. Okumura, and Y. Yasui, Field evolution of magnetic phases and spin dynamics in the honeycomb lattice magnet $Na_2Co_2TeO_6$: ^{23}Na NMR study, Phys. Rev. B **106**, 224416 (2022).

[61] L. Viciu, Q. Huang, E. Morosan, H. Zandbergen, N. Greenbaum, T. McQueen, and R. Cava, Structure and basic magnetic properties of the honeycomb lattice compounds $Na_2Co_2TeO_6$ and $Na_3Co_2SbO_6$, J. Solid State Chem. **180**, 1060 (2007).

[62] E. Lefrançois, M. Songvilay, J. Robert, G. Nataf, E. Jordan, L. Chaix, C. V. Colin, P. Lejay, A. Hadj-Azzem, R. Ballou, and V. Simonet, Magnetic properties of the honeycomb oxide $Na_2Co_2TeO_6$, Phys. Rev. B **94**, 214416 (2016).

[63] A. K. Bera, S. M. Yusuf, A. Kumar, and C. Ritter, Zigzag antiferromagnetic ground state with anisotropic correlation lengths in the quasi-two-dimensional honeycomb lattice compound $Na_2Co_2TeO_6$, Phys. Rev. B **95**, 094424 (2017).

[64] F. Ye, S. Chi, H. Cao, B. C. Chakoumakos, J. A. Fernandez-Baca, R. Custelcean, T. F. Qi, O. B. Korneta, and G. Cao, Direct evidence of a zigzag spin-chain structure in the honeycomb lattice: A neutron and x-ray diffraction investigation of single-crystal Na_2IrO_3, Phys. Rev. B **85**, 180403(R) (2012).

[65] J. A. Sears, M. Songvilay, K. W. Plumb, J. P. Clancy, Y. Qiu, Y. Zhao, D. Parshall, and Y.-J. Kim, Magnetic order in α-$RuCl_3$: A honeycomb-lattice quantum magnet with strong spin-orbit coupling, Phys. Rev. B **91**, 144420 (2015).

[66] H. B. Cao, A. Banerjee, J.-Q. Yan, C. A. Bridges, M. D. Lumsden, D. G. Mandrus, D. A. Tennant, B. C. Chakoumakos, and S. E. Nagler, Low-temperature crystal and magnetic structure of α-$RuCl_3$, Phys. Rev. B **93**, 134423 (2016).

[67] M. Gillig, X. Hong, C. Wellm, V. Kataev, W. Yao, Y. Li, B. Büchner, and C. Hess, Phononic-magnetic dichotomy of the thermal Hall effect in the Kitaev-Heisenberg candidate material $Na_2Co_2TeO_6$, arXiv:2303.03067.

[68] W. G. F. Krüger, W. Chen, X. Jin, Y. Li, and L. Janssen, Triple-Q order in $Na_2Co_2TeO_6$ from proximity to hidden-SU(2)-symmetric point, arXiv:2211.16957 (2022).

[69] O. Heinonen, R. A. Heinonen, and H. Park, Magnetic ground states of a model for $M Nb_3S_6 (M = \mathrm{Co, Fe, Ni})$, Phys. Rev. Mater. **6**, 024405 (2022).

[70] Y. Yanagi, H. Kusunose, T. Nomoto, R. Arita, and M.-T. Suzuki, Generation of modulated magnetic structures based on cluster multipole expansion: Application to α-Mn and CoM_3S_6, Phys. Rev. B **107**, 014407 (2023).

[71] See Supplemental Material at http://link.aps.org/supplemental/10.1103/PhysRevResearch.5.L022045 for additional methods, data, and analyses, which includes Refs. [43,78–83].

[72] C. Balz, L. Janssen, P. Lampen-Kelley, A. Banerjee, Y. H. Liu, J.-Q. Yan, D. G. Mandrus, M. Vojta, and S. E. Nagler, Field-induced intermediate ordered phase and anisotropic interlayer interactions in α-$RuCl_3$, Phys. Rev. B **103**, 174417 (2021).

[73] X. Zhang, Y. Xu, T. Halloran, R. Zhong, C. Broholm, R. Cava, N. Drichko, and N. Armitage, A magnetic continuum in the cobalt-based honeycomb magnet $BaCo_2(AsO_4)_2$, Nat. Mater. **22**, 58 (2023).

[74] X. Liu and H.-Y. Kee, Non-Kitaev versus Kitaev honeycomb cobaltates, Phys. Rev. B **107**, 054420 (2023).

[75] R. D. Johnson, S. C. Williams, A. A. Haghighirad, J. Singleton, V. Zapf, P. Manuel, I. I. Mazin, Y. Li, H. O. Jeschke, R. Valentí, and R. Coldea, Monoclinic crystal structure of α-$RuCl_3$ and the zigzag antiferromagnetic ground state, Phys. Rev. B **92**, 235119 (2015).

[76] L. Spitz, T. Nomoto, S. Kitou, H. Nakao, A. Kikkawa, S. Francoual, Y. Taguchi, R. Arita, Y. Tokura, T.-H. Arima, and M. Hirschberger, Entropy-assisted, long-period stacking of honeycomb layers in an AlB_2-type silicide, J. Am. Chem. Soc. **144**, 16866 (2022).

[77] X. Jin, G. He, C. Balz, W. Yao, Y. Li, and X. Li (2021), Investigation of spin excitations in $Na_2Co_2TeO_6$ single crystals, STFC ISIS Neutron and Muon Source, https://doi.org/10.5286/ISIS.E.RB2010025.

[78] J. Lynn, Y. Chen, S. Chang, Y. Zhao, S. Chi, W. Ratcliff, B. G. Ueland, and R. W. Erwin, Double-focusing thermal triple-axis spectrometer at the NCNR, J. Res. Natl. Inst. Stand. Technol. **117**, 60 (2012).

[79] J. A. Rodriguez, D. M. Adler, P. C. Brand, C. Broholm, J. C. Cook, C. Brocker, R. Hammond, Z. Huang, P. Hundertmark, J. W. Lynn, N. C. Maliszewskyj, J. Moyer, J. Orndorff, D. Pierce, T. D. Pike, G. Scharfstein, S. A. Smee, and R. Vilaseca, MACS—a new high intensity cold neutron spectrometer at NIST, Meas. Sci. Technol. **19**, 034023 (2008).

[80] R. Bewley, J. Taylor, and S. Bennington, LET, a cold neutron multi-disk chopper spectrometer at ISIS, Nucl. Instrum. Methods Phys. Res., Sect. A **637**, 128 (2011).

[81] R. T. Azuah, L. R. Kneller, Y. Qiu, P. L. Tregenna-Piggott, C. M. Brown, J. R. Copley, and R. M. Dimeo, DAVE: A comprehensive software suite for the reduction, visualization, and analysis of low energy neutron spectroscopic data, J. Res. Natl. Inst. Stand. Technol. **114**, 341 (2009).

[82] R. Ewings, A. Buts, M. Le, J. Van Duijn, I. Bustinduy, and T. Perring, Horace: Software for the analysis of data from single crystal spectroscopy experiments at time-of-flight neutron instruments, Nucl. Instrum. Methods Phys. Res., Sect. A **834**, 132 (2016).

[83] G. Shirane, S. M. Shapiro, and J. M. Tranquada, *Neutron Scattering with a Triple-Axis Spectrometer: Basic Techniques* (Cambridge University Press, Cambridge, UK, 2002).